Journal of Biomolecular NMR (2005) 31: 49–57

TEDOR with adiabatic inversion pulses: Resonance assignments of $^{13}C/^{15}N$ labelled RNAs

Kerstin Riedel, Jörg Leppert, Oliver Ohlenschläger, Matthias Görlach & Ramadurai Ramachandran*

Abteilung Molekulare Biophysik/NMR-Spektroskopie, Institut für Molekulare Biotechnologie, 07745 Jena, Germany

Received 16 September 2004; Accepted 22 October 2004

Key words: adiabatic pulse, MAS, RNA, solid state NMR, TEDOR

Abstract

We have examined via numerical simulations the performance characteristics of different ^{15}N RF pulse schemes employed in the transferred echo double resonance (TEDOR) experimental protocol for generating ^{13}C–^{15}N dipolar chemical shift correlation spectra of isotopically labelled biological systems at moderate MAS frequencies ($\omega_r \sim 10$ kHz). With an ^{15}N RF field strength of ~30–35 kHz that is typically available in 5 mm triple resonance MAS NMR probes, it is shown that a robust TEDOR sequence with significant tolerance to experimental imperfections such as H_1 inhomogeneity and resonance offsets can be effectively implemented using adiabatic heteronuclear dipolar recoupling pulse schemes. TEDOR-based ^{15}N–^{13}C and ^{15}N–^{13}C–^{13}C chemical shift correlation experiments were carried out for obtaining ^{13}C and ^{15}N resonance assignments of an RNA composed of 97 (CUG) repeats which has been implicated in the neuromuscular disease myotonic dystrophy.

Introduction

Magic angle spinning (MAS) solid state NMR is emerging as an important tool for the structural characterisation of biological systems that are not easily amenable for solution state NMR or X-ray crystallographic investigations. Employing a set of MAS NMR derived approximate distance constraints, Castellani et al. (2002) have demonstrated recently the possibilities for obtaining biomolecular structures in the solid state. The pre-requisite for MAS NMR-based structural investigation, as in solution state NMR, is the assignment of resonances and homo- and heteronuclear chemical shift correlation experiments are commonly employed for this. Although dipolar interactions between low γ nucleiare typically averaged out under MAS conditions, a variety of techniques have been reported for inhibiting such spatial averaging of weak dipolar couplings (Bennett et al., 1994; Griffin, 1998; Dusold and Sebald, 2000) and for generating efficient *dipolar* chemical shift correlation spectra (Sun et al., 1997; Rienstra et al., 2000; Detken et al., 2001; Pauli et al., 2001; Baldus, 2002; Castellani et al., 2003). 2D transferred echo double resonance (TEDOR) is one of the simplest techniques for obtaining ^{13}C–^{15}N (*I*–*S*) dipolar chemical shift correlation spectra of biological systems (Hing et al., 1992). The possibilities for the simultaneous measurement of multiple carbon–nitrogen distances in uniformly $\{^{13}C, ^{15}N\}$ labelled systems via the TEDOR approach have also been demonstrated recently by Jaroniec et al. (2002). Different variants of 2D TEDOR RF pulse scheme have been reported (Van Eck and Veeman, 1994; Michal and Jelinski, 1997; Jaroniec et al., 2002).

*To whom correspondence should be addressed. E-mail: raman@imb-jena.de

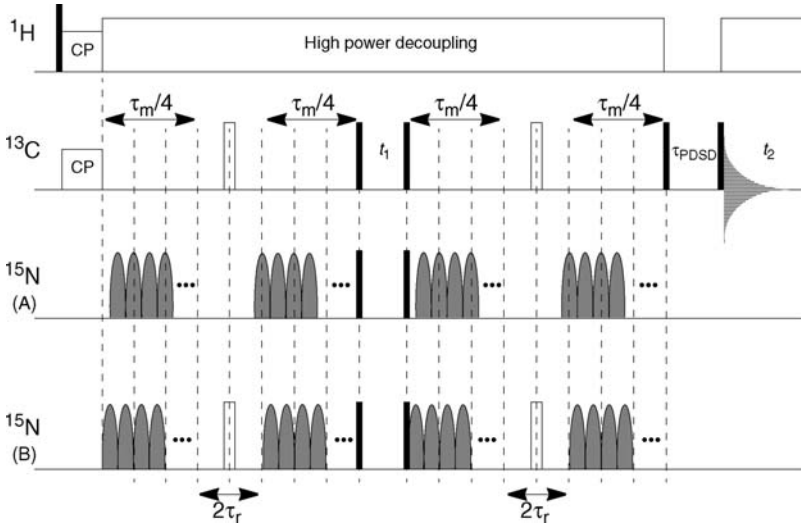

Figure 1. TEDOR pulse sequence employed in this work. In the conventional approach two ^{15}N inversion pulses per rotor period were applied, centred at the middle and end of the rotor period (a). Simultaneous (^{15}N, ^{13}C) π pulses were applied at the centre of the dipolar recoupling periods in the TEDOR protocol employing symmetry-based ^{15}N RF irradiation (b). After the TEDOR step, proton-driven spin diffusion was used to induce longitudinal magnetisation transfers from ^{15}N attached ^{13}C nuclei to other carbons. By standard phase cycling procedures the desired coherence transfer pathways were selected and 2D phase sensitive spectra were generated.

The sequence employed in this work (Figure 1) essentially involves, as in earlier studies (Michal and Jelinski, 1997; Jaroniec et al., 2002), the creation of the anti-phase operator term I_yS_z starting with an initial in-phase operator term I_x. The I_yS_z term is then converted to the term S_xI_z via the simultaneous application of I, S $\pi/2$ pulses. The S-spin magnetisation (S_xI_z) is frequency labelled in the t_1 dimension and converted back to the I_yS_z term via the simultaneous application of a second pair of I, S $\pi/2$ pulses, as in 2D HSQC experiments of solution state NMR. The anti-phase term I_yS_z is then converted back to the I_x term and the I spins are frequency labelled in the t_2 dimension. The conversions $I_x \leftrightarrow I_yS_z$ are achieved by the application of suitable heteronuclear dipolar recoupling pulse sequences. For minimising the effects of ^{13}C–^{13}C dipolar couplings and ^{13}C/^{15}N CSA interactions on the TEDOR performance characteristics in uniformly {^{13}C,^{15}N} labelled biological systems, Jaroniec et al. (2002) have pointed out that it is advantageous to achieve heteronuclear dipolar recoupling via a suitable RF pulse sequence applied entirely on the S-spin (^{15}N) channel and with only a single I-spin π pulse applied at the middle of the dipolar recoupling period to refocus I-spin isotropic chemical shift evolution.

Heteronuclear dipolar recoupling in TEDOR is normally achieved, as in rotational echo double resonance (REDOR) experiments (Gullion and Schaefer, 1989), via the application of rotor-synchronised rectangular π pulses. However, the performance characteristics of multiple pulse NMR sequences involving the repeated application of conventional rectangular π pulses are affected by experimental imperfections such as flip angle errors arising from difficulties in pulse length calibration with low-sensitivity samples, H_1 inhomogeneities and resonance offsets (Naito et al., 1996; Nishimura et al., 2001; Weldeghiorghis and Schaefer, 2003; Sinha et al., 2004). Additionally, amplifier and/or probe instabilities can contribute to fluctuations in the RF field strength and lead to degradation in the performance of the multiple pulse NMR sequences. Consideration of the effects of experimental imperfections are particularly important when extended heteronuclear dipolar recoupling periods are employed, for example in long range ^{13}C–^{15}N distance measurement studies. In view of the fact that TEDOR-based MAS NMR pulse schemes hold considerable potential in the study of isotopically labelled biological systems (Fujiwara et al., 1995; Hong and Griffin, 1998; Hong, 1999; Jaroniec et al., 2002), both for

resonance assignments and for distance measurements, it will be advantageous if a robust TEDOR scheme that is relatively insensitive to experimental imperfections can be implemented employing the limited ^{15}N RF field strength (~30–35 kHz) typically available in 5 mm MAS triple resonance probes. In this context it is worth noting that recent studies in a variety of MAS NMR experiments have shown that it is possible to effectively minimise the deleterious effects of H_1 inhomogeneities and resonance offsets via the usage of adiabatic inversion pulses instead of conventional rectangular pulses (Heise et al., 2002; Leppert et al., 2002, 2003, 2004a; Hardy et al., 2003; Riedel et al., 2004a). Encouraged by the results obtained in these studies we have examined via numerical simulations the TEDOR performance characteristics of different adiabatic ^{15}N RF pulse phasing schemes, including CN_n^v symmetry-based heteronuclear dipolar recoupling schemes recently proposed by Chan and Eckert (2001) based on the works of Levitt and co-workers (Carravetta et al., 2000; Brinkmann and Levitt, 2001; Levitt, 2002).

2D adiabatic TEDOR-based ^{15}N–^{13}C and ^{15}N–^{13}C–^{13}C chemical shift correlation experiments were carried out on the CUG triplet repeat expansion RNA $(CUG)_{97}$ (mol. wt ~100 kDa) that has been implicated in the neuromuscular disease myotonic dystrophy (Ranum and Day, 2004). Structural studies of RNAs are typically carried out via solution state NMR investigations. However the study of large RNA systems via solution state NMR techniques is difficult, if not impossible. The line widths of the NMR resonances seen in the solution state increase with increase in the size of the system studied and make RNA resonance assignments difficult. To overcome this RNA size bottleneck, we are currently exploring the potential of MAS solid state NMR for the study of RNAs, as the linewidth observed in the solid state is not dependent on the size of the molecule. Our recent studies with $(CUG)_{97}$ suggest that it is possible to investigate very large RNA systems via MAS solid state NMR (Leppert et al., 2004b). 2D ^{15}N dipolar correlation experiments with $(CUG)_{97}$ have shown the presence of NH···N hydrogen bond involving GN_1 and CN_3 nitrogens, corresponding to a canonical GC Watson–Crick base-pairing scheme. In this study, we have obtained ^{13}C and ^{15}N resonance assignments of $(CUG)_{97}$ via heteronuclear dipolar chemical shift correlation experiments and the results from these investigations are also presented below.

Numerical and experimental procedures

Numerical simulations were carried out using the SIMPSON program (Bak et al., 2000) considering two spin-1/2 heteronuclei (*I–S*) and a Zeeman field strength of 11.7 T. The performance characteristics of different ^{15}N RF pulse schemes were assessed by monitoring as a function of the net heteronuclear dipolar recoupling period (τ_m) the magnitude of the *I*-spin (^{13}C) magnetisation observed at $t_0 = 0$. In this study we have employed tan h/tan adiabatic inversion pulses (Hwang et al., 1998) constructed from the following adiabatic half passage and its time reversed half passage:

$$\omega_1(t) = \omega_1(\max)\tan h[\xi 2t/T_p]$$

$$\Delta\omega(t) = \Delta\omega_{max}[\tan(\kappa(1 - 2t/T_p))]/\tan(\kappa),$$

where $\xi = 10$, $\tan(\kappa) = 20$ and $0 \le t \le T_p/2$. The frequency sweep is implemented in the spectrometer hardware as a phase modulation, $\phi(t) = \int\Delta\omega(t)dt$.

Adiabatic pulses with durations, power levels and phasing scheme as given in the figure captions were employed. All tanh/tan pulses used in this work had a pulse bandwidth and pulse length product value of 60 (Hwang et al., 1998). Experiments were carried out at a spinning speed of 10,000 Hz with an undiluted, fully hydrated $\{^{15}N,^{13}C\}$ labelled sample of $(CUG)_{97}$ at ~−15°C on a 500 MHz wide-bore Varian ^{UNITY}*INOVA* solid state NMR spectrometer equipped with a 5 mm DOTY supersonic triple resonance probe and a waveform generator for pulse shaping. The $\{^{15}N,^{13}C\}$ labelled RNA sample was prepared from $\{^{15}N,^{13}C\}$ labelled NTPs as described earlier (Leppert et al., 2004b). Cross-polarisation under Hartmann–Hahn matching conditions was employed and all spectra, unless mentioned otherwise, were collected under high power ^{1}H decoupling (~90 kHz). Typical ^{1}H, ^{15}N and ^{13}C 90° pulse widths were 2.8, 8.0 and 7.8 μs, respectively. Other details are given in the figure captions.

Results and discussion

We have evaluated the RF field strength requirements and the performance of different dipolar recoupling sequences applied to the ^{15}N channel at a representative spinning speed of 10 kHz, unless mentioned otherwise. To assess the relative merits of different pulse schemes clearly, a weak ^{13}C–^{15}N dipolar coupling strength of 190 Hz was employed in these simulations. The effects of CSAs were neglected, unless mentioned otherwise. Simulations were carried out employing both conventional and symmetry-based heteronuclear dipolar recoupling RF pulse schemes. In the conventional approach two ^{15}N inversion pulses per rotor period were applied, centred at the middle and end of the rotor period (Figure 1a). To reduce RF power requirements the duration of the adiabatic pulses were set to correspond to 50% of the rotor period. CN_n^v symmetry-based heteronuclear dipolar recoupling sequences were generated with adiabatic inversion pulses employing basic *C* elements $\{x\bar{x}\}$ and$\{xx\bar{x}\bar{x}\}$, with *x* and $\bar{x}$ representing π pulses with x and −x phases. To ensure additive dipolar evolution of the *I*-spin magnetisation (Chan and Eckert, 2001), simultaneous (^{15}N, ^{13}C) π pulses were applied at the centre of the heteronuclear dipolar recoupling periods in the TEDOR sequence employing symmetry-based dipolar recoupling irradiation (Figure 1b). Except for the ^{15}N pulses applied during the dipolar recoupling periods, all RF pulses were assumed to be δ pulses in the numerical calculations. As the aromatic ^{15}N resonances of RNAs span a much larger isotropic chemical shift range (~170 ppm), unlike the backbone ^{15}N resonances of peptide/protein, simulations were also carried out considering a ^{15}N resonance offset range of ± 5 kHz. For comparison, the simulated TEDOR plots generated with rectangular pulse-based ^{15}N RF irradiations, including those obtained with $\sim \pm 10\%$ variation in the RF field strength, are also given below. Unless mentioned otherwise, TEDOR plots were generated using the conventional ^{15}N RF irradiation scheme given in Figure 1a.

Simulated TEDOR plots generated as a function of the RF field strength employing different ^{15}N RF irradiation schemes are given in Figure 2. When the available ^{15}N RF field strength is limited, as in our case, and when one deals with a large ^{15}N resonance offset range, the TEDOR performance with rectangular pulses employing the *xy*-4 phasing scheme (Gullion et al., 1990) is found to be not satisfactory in the presence of H_1 inhomogeneities (Figure 2a). On the other hand, it is possible to obtain (Figure 2b) relatively better TEDOR performance with adiabatic inversion pulses employing the m4 $\{xx\bar{x}\bar{x}\}$ phasing scheme (Levitt et al., 1983). Although the adiabatic inversion pulses occupy a significant fraction of the rotor period, Figure 2b shows, in agreement with our earlier study (Leppert et al., 2002), that satisfactory heteronuclear dipolar recoupling can be achieved with adiabatic pulses. Figure 2c shows the TEDOR plots obtained with the m4 phasing scheme and a ^{15}N RF field strength of 30 kHz. It is seen that the improved TEDOR performance with adiabatic pulses is obtained without sacrificing the sensitivity of the initial rate of build up of the *I*-spin intensities to the heteronuclear dipolar coupling strength and hence to the internuclear distance involved. In addition, the TEDOR performance is not significantly affected by ^{15}N CSAs (Figure 2c). Compared to the *xy*-4 phasing scheme, improved TEDOR performance can be obtained (Figure 2d) with rectangular pulses employing the *xy*-8 phasing scheme (Gullion et al., 1990). For the same number of rotor periods required for the implementation of the *xy*-8 phasing scheme one can obtain (Figure 2e) superior TEDOR performance with adiabatic pulses employing the m8 $\{xx\bar{x}\bar{x}x\bar{x}\bar{x}x\}$ phasing scheme (Levitt et al., 1983). The TEDOR performance with adiabatic pulses under the *xy*-8 phasing scheme (data not shown) is also comparable to that shown in Figure 2e. Even at a spinning speed of 12,500 Hz it is possible to obtain satisfactory adiabatic TEDOR performance characteristics employing tan h/tan adiabatic pulses of 40 μs duration and with ^{15}N RF field strength of ~30–35 kHz (Figure 2f). The TEDOR performance observed with symmetry-based heteronuclear dipolar recoupling schemes is depicted in Figures 2g–i. For CN_n^v sequences employing rectangular RF pulses the RF field strength required is related to the spinning frequency as $(\omega_1/\omega_r) = (N/n)(\tau_c/\tau_{2\pi})$, where τ_c and $\tau_{2\pi}$ represent the length of the *C* element and a 2π pulse, respectively. Hence, the simulations shown in Figure 2g, generated with the $C3_3^1$ symmetry-based heteronuclear dipolar recoupling scheme employing the POST *C* element $\{(\pi/2)_0(2\pi)_\pi(3\pi/2)_0\}$ (Chan et al.,

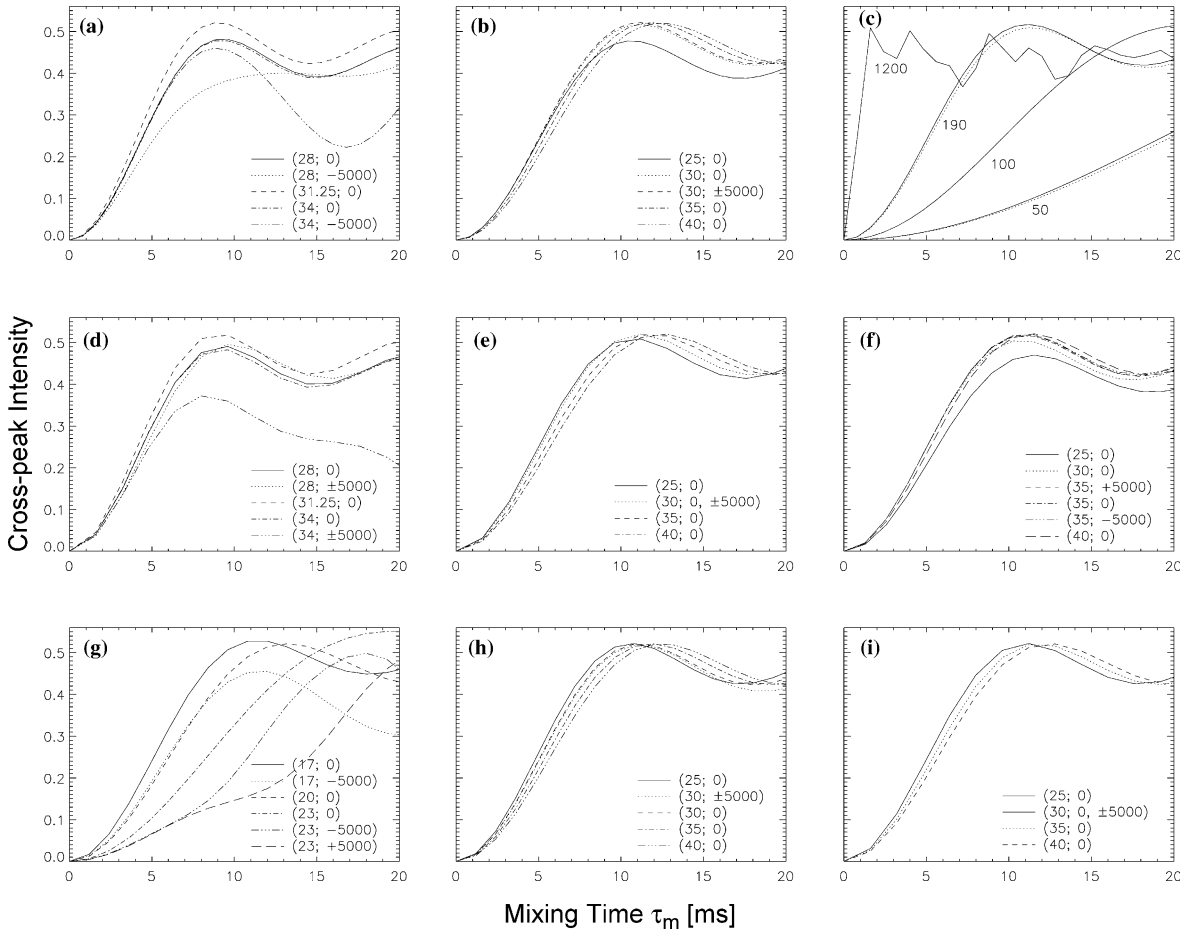

Figure 2. Simulated TEDOR plots ($\omega_r = 10{,}000$ Hz) generated with different ^{15}N RF irradiation schemes employing a ^{13}C–^{15}N dipolar coupling strength of 190 Hz and neglecting ^{15}N and ^{13}C CSAs, unless indicated otherwise. The two numbers shown corresponding to each of the plots represent, respectively, the RF field strength (kHz) and the resonance offsets (Hz) employed in the simulations. Euler angles defining the orientation of CS tensors $\Omega_{1,2}$ in an arbitrary molecular frame were fixed at (0°, 0°, 0°) and the orientation of the dipolar vector in the molecular frame was fixed at (0°, 0°). (a) rectangular inversion pulses (16 μs, *xy*-4 phasing scheme), (b) adiabatic inversion pulses (50 μs, m4 {xx$\bar{x}\bar{x}$} phasing scheme), (c) adiabatic pulses with m4 phasing scheme and as a function of the ^{13}C–^{15}N dipolar coupling strength (Hz) indicated, with (shift anisotropy $\delta_{aniso}(N) = 106.0$ ppm, asymmetry parameter $\eta(N) = 0.27$, dotted line) and without ^{15}N CSA, (d) rectangular inversion pulses (16 μs, *xy*-8 phasing scheme), (e) adiabatic pulses with m8 {xx$\bar{x}\bar{x}$xx$\bar{x}\bar{x}$x} phasing scheme, (f) adiabatic pulses (40 μs) with m8 phasing scheme at a spinning speed of 12,500 Hz, (g) $C3_3^1$ symmetry-based heteronuclear dipolar recoupling scheme employing the POST *C* element {$(\pi/2)_0(2\pi)_\pi(3\pi/2)_0$}, (h) $C3_3^1$ symmetry-based adiabatic heteronuclear dipolar recoupling scheme with the basic *C* element {x$\bar{x}$} and (i) $C2_4^1$ symmetry-based adiabatic heteronuclear dipolar recoupling scheme with the basic *C* element {xx$\bar{x}\bar{x}$}.

2001), were carried out with ^{15}N RF field strengths centred at 20 kHz. They indicate that in the presence of H_1 inhomogeneities and resonance offsets the TEDOR performance is not satisfactory. On the other hand, good TEDOR performance can be obtained employing adiabatic symmetry-based dipolar recoupling schemes $C3_3^1$ (Figure 2h) and $C2_4^1$(Figure 2i). It is worth noting that unlike the restriction in the case of rectangular pulses, the RF field strength required in symmetry-based schemes involving adiabatic inversion pulses is not related to the spinning speed. This facilitates the effective application of symmetry-based RF pulse schemes to lower MAS frequency regime also.

Simulations carried out considering a three spin dipolar network of the type IS_2 showed that the TEDOR transfer characteristics seen with adiabatic symmetry-based schemes mentioned above are affected by the presence of strong homonuclear dipolar couplings (data not shown).

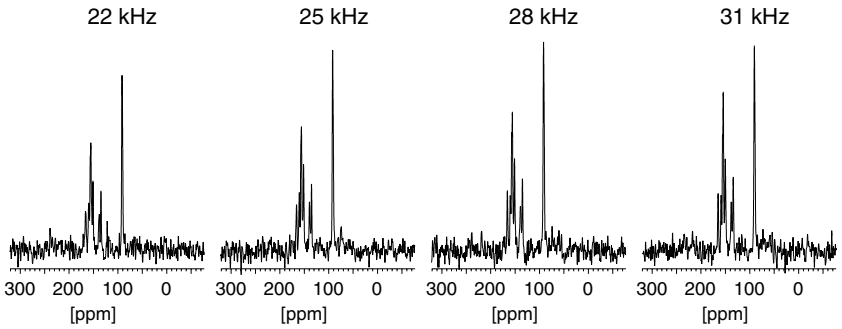

Figure 3. ^{13}C TEDOR signals of $(CUG)_{97}$ obtained ($t_1 = 0$, $\tau_m = 1.6$ ms, $\omega_r = 10{,}000$ Hz, 512 transients, 2 ms CP contact time, 2.5 s recycle time) as a function of the ^{15}N RF field strength indicated employing tan*h*/tan adiabatic pulses of 50 μs duration, m4 phasing scheme and as per conventional ^{15}N dipolar recoupling irradiation shown in Figure 1a.

In addition to the allowed terms in the average Hamiltonian of the sequence $C3_3^1$, the $C2_4^1$ scheme allows additional homonuclear dipolar coupling terms. However, since ^{15}N–^{15}N dipolar couplings are weak these couplings were not considered in this study. It is also worth mentioning that the adiabatic TEDOR performance seen in Figure 2h is significantly better than that obtained with adiabatic RF irradiation as per Figure 1a and employing the simple phasing scheme $\{x\bar{x}\}$ (data not shown). In addition to the simulations given in Figure 2 we have also carried out numerical simulations with ^{15}N RF irradiations employing supercycles such as *xy*-16 (Gullion et al., 1990) and (p5d)(m4) (Levitt et al., 1983; Tycko et al., 1985; Leppert et al., 2003) and obtained improved TEDOR performance characteristics (data not shown). However at lower MAS frequencies and in the presence of strong heteronuclear dipolar interactions the implementation of such schemes, requiring a large number of rotor periods, may not be possible as it will be difficult to collect sufficient number of data points in the initial cross-peak build up region of the TEDOR curve. Initial studies indicate that it is also possible to generate satisfactory TEDOR performance characteristics employing RN_n^v symmetry-based adiabatic dipolar recoupling sequences (data not shown). To assess only the relative performance of different heteronuclear dipolar recoupling schemes, we have assumed δ pulse characteristics for the ^{15}N π pulses applied at the centre of the symmetry-based dipolar recoupling RF irradiation (Figure 1b). The results of our numerical simulations (Figure 2) clearly indicate that at moderate MAS frequencies it is possible to carry out efficient heteronuclear dipolar recoupling with different conventional and symmetry-based adiabatic RF pulse schemes employing ^{15}N RF field strength of ~30–35 kHz and obtain improved TEDOR performance. From these data, it is clear that the TEDOR performance obtained with conventional adiabatic heteronuclear dipolar recoupling irradiation (Figure 1a) is comparable to that of the symmetry-based scheme (Figure 1b). However, when only a limited ^{15}N RF field strength is available, the overall performance of TEDOR under symmetry-based RF irradiation will be affected by the performance characteristics of the additional ^{15}N π pulses. In this context, it may be advantageous to implement TEDOR with conventional adiabatic heteronuclear dipolar recoupling via the scheme given in Figure 1a.

We have carried out adiabatic TEDOR-based ^{13}C–^{15}N chemical shift correlation experiments as per scheme in Figure 1a and obtained ^{13}C and ^{15}N resonance assignments for the CUG triplet repeat expansion RNA. Figure 3 shows for $t_1 = 0$, and as a function of the ^{15}N RF field strength, the ^{13}C signals obtained ($\omega_r = 10000$ Hz) employing tan*h*/tan adiabatic pulses of 50 μs duration and the m4 phasing scheme. The ^{15}N RF field strength dependence is in satisfactory agreement with the results obtained from numerical simulations. The 2D ^{13}C–^{15}N chemical shift correlation spectrum obtained using a proton-driven spin diffusion (PDSD) (Szeverenyi et al., 1982) mixing time of zero is shown in Figure 4. This spectrum shows all the expected heteronuclear correlations and characteristic connectivity patterns for the different

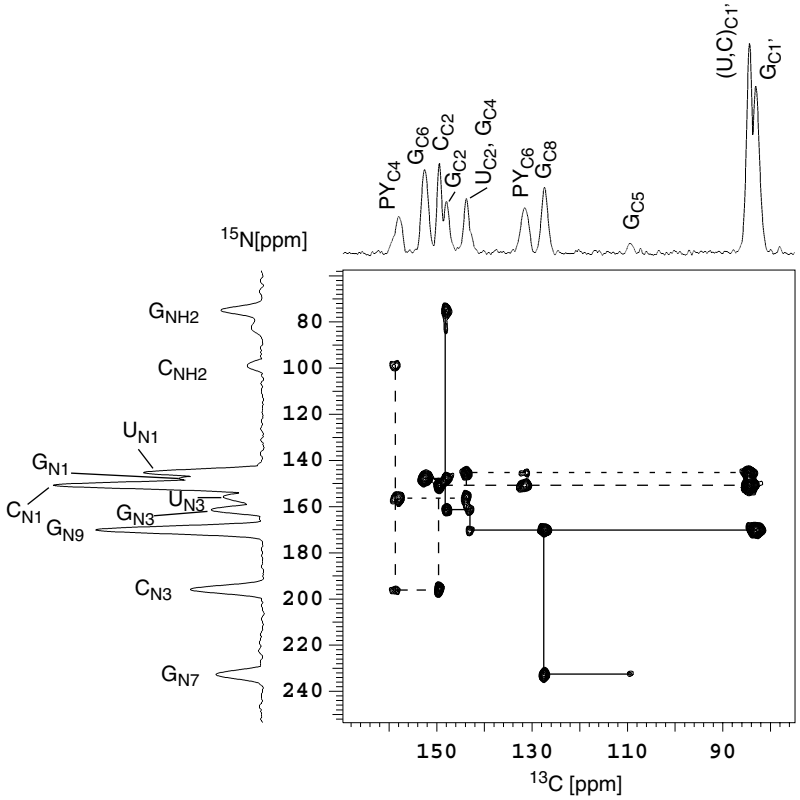

Figure 4. The 2D ^{13}C–^{15}N chemical shift correlation spectra of $(CUG)_{97}$ obtained ($\tau_m = 1.6$ ms, $\omega_r = 10{,}000$ Hz, 128 transients, 2 ms CP contact time, 2.5 s recycle time, 57 t_1 increments, ω_1 spectral width of 10,000 Hz, PDSD mixing time of zero) using a ^{15}N RF field strength of ~31 kHz. Other parameters employed are as in Figure 3. ^{15}N chemical shifts are referenced with respect external solid NH_4Cl ($\delta_N = 38.5$ ppm with respect to liquid NH_3) and ^{13}C chemical shifts are referenced with respect to external adamantane ($\delta_{CH} = 29.5$ ppm with respect to TMS).

nucleotides. The assignments given on the spectral projections are based on the observed connectivity patterns. They are consistent with the expected isotropic chemical shifts in solution state NMR studies of RNAs (Wijmenga and van Buuren, 1998). The 2D spectrum, generated with a short τ_m value, does not show correlations arising from carbons not directly connected to nitrogen nuclei. To obtain complete assignment of all the ^{13}C nuclei in $(CUG)_{97}$, we have carried out 2D ^{15}N–^{13}C–^{13}C chemical shift correlation experiments with PDSD (50 ms) to achieve longitudinal magnetisation exchange from ^{13}C nuclei directly bonded to ^{15}N to other remote carbons (e.g. $^{15}N_{1,9} \rightarrow C1' \rightarrow C2'$, C3′, C4′ and C5′ & $^{15}N_{1,9} \rightarrow C6 \rightarrow C5$). Figure 5A shows the 2D ^{15}N–^{13}C correlation spectrum ($^{15}N_1$ and $^{15}N_9$ region) obtained employing a short CP contact time of ~100 μs and with a PDSD mixing time of zero. Due to the short CP contact time, only the carbons that are directly connected to ^{1}H nuclei are preferentially seen in this ^{13}C–^{15}N heteronuclear correlation spectrum. Figure 5b shows the heteronuclear correlation spectrum obtained with a PDSD mixing time of 50 ms. Due to the very small isotropic chemical shift dispersion of the sugar carbon resonances, PDSD is very efficient in transferring magnetisation from the C1′ carbons to other sugar carbons. Collection of data employing short values for the PDSD mixing time permits the assignment of all sugar carbon resonances. The assignments of the sugar and aromatic carbon resonances shown on the spectral projection are consistent with our recent ^{13}C–^{13}C 2D homonuclear dipolar correlation experiments on $(CUG)_{97}$ (Riedel et al., 2004b). Spectrum 5B also shows cross-peaks arising from magnetisation exchange involving aromatic carbons. For example the C5

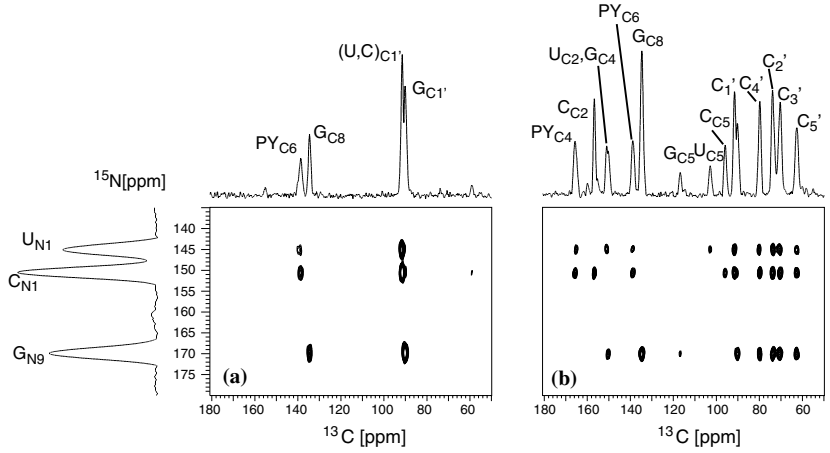

Figure 5. 2D ^{15}N–^{13}C correlation spectra ($^{15}N_1$ and $^{15}N_9$ region) obtained with a PDSD mixing time of zero (a) and 50 ms (b). Spectra A ($\tau_m = 1.6$ ms, $\omega_r = 10{,}000$ Hz, 64 transients, 110 μs CP contact time, 2.5 s recycle time, 64 t_1 increments, ω_1 spectral width of 10,000 Hz) and B ($\tau_m = 1.6$ ms, $\omega_r = 10{,}000$ Hz, 512 transients, 110 μs CP contact time, 1 s recycle time, 96 t_1 increments, ω_1 spectral width of 10,000 Hz) were generated with tan*h*/tan adiabatic pulses as in Figure 4.

carbon resonances belonging to the pyrimidine bases and arising from C6 → C5 magnetisation transfers can be clearly seen.

The results presented in this study clearly indicate that TEDOR with adiabatic heteronuclear dipolar recoupling schemes allows conveniently to group all the resonances belonging to the same nucleotide residue in an RNA. This should facilitate the analysis of ^{13}C chemical shifts of each nucleotide residue in structural terms (Ebrahimi et al., 2001; Riedel et al., 2004b). In the study of many biological systems, unless experiments can be carried out at very low temperatures, it may be difficult to use very high spinning speeds, for example to avoid sample dehydration. Hence, in this current work we have examined the efficacy of adiabatic TEDOR at a moderate MAS frequency of 10 kHz. However, in situations where it is possible to use higher MAS frequencies, it should be feasible to implement adiabatic TEDOR for generating heteronuclear correlation spectra. However such studies would require the availability of higher ^{15}N RF field strengths, for example as available in MAS NMR probes with smaller rotor diameter. As in the recent study of Jaroniec et al. (2002), it is also possible to carry out band-selective TEDOR experiments in the study of isotopically labelled RNAs, for example to monitor selectively the correlations originating from either the sugar or aromatic carbon resonances. In addition to the tan*h*/tan adiabatic pulses employed in this work other suitable adiabatic pulses could also be applied in these studies. The fact that the isotropic chemical shifts observed in the solid state is similar to that obtained in typical solution state NMR RNA studies suggests that, in favourable situations, it may be possible to exploit the potential of both the methods in the structural characterisation of RNA systems. To facilitate the structural characterisation of $(CUG)_{97}$, we have undertaken first the assignment of ^{13}C and ^{15}N resonances via ^{15}N–^{13}C chemical shift correlation experiments. Studies dealing with long range ^{13}C–^{15}N distance measurements are planned. The results presented here clearly indicate that it should be feasible to perform MAS solid state NMR-based structural studies of complex RNA systems with large molecular weights employing suitable segement, base and strand specific isotopic labelling strategies.

References

Bak, M., Rasmussen, J.T. and Nielsen, N.C. (2000) *J. Magn. Reson.*, **147**, 296–330.

Baldus, M. (2002) *Prog. NMR Spectrosc.*, **41**, 1–47.

Bennett, A.E., Griffin, R.G. and Vega, S. (1994) *NMR Basic Principles and Progress*, Vol. 33, Springer Verlag, Berlin, pp. 1–77.

Brinkmann, A. and Levitt, M.H. (2001) *J. Chem. Phys.*, **115**, 357–384.

Carravetta, M., Eden, M., Zhao, X., Brinkmann, A. and Levitt, M.H. (2000) *Chem. Phys. Lett.*, **321**, 205–215.
Castellani, F., van Rossum, B., Diehl, A.M., Rehbein, K. and Oschkinat, H. (2003) *Biochemistry*, **42**, 11476–11483.
Castellani, F., van Rossum, B., Diehl, A., Schubert, M., Rehbein, K., and Oschkinat, H. (2002) *Nature*, **420**, 98–102.
Chan, J.C.C. and Eckert, H. (2001) *J. Chem. Phys.*, **115**, 6095–6105.
Detken, A., Hardy, E.H., Ernst, M., Kainosho, M., Kawakami, T., Aimoto, S. and Meier, H.M. (2001) *J. Biomol. NMR*, **20**, 203–221.
Dusold, S. and Sebald, A. (2000) *Annu. Rep. NMR Spectrosc.*, **41**, 185–264.
Ebrahimi, M., Rossi, P., Rogers, C. and Harbison, G.S. (2001) *J. Magn. Reson.*, **150**, 1–9.
Fujiwara, T., Sugase, K., Kainosho, M., Ono, A., Ono, A.M. and Akutsu, H. (1995) *J. Am. Chem. Soc.*, **117**, 11351–11352.
Griffin, R.G. (1998) *Nat. Struct. Biol.*, **5**, 508–512.
Gullion, T. and Schaefer, J. (1989) *J. Magn. Reson.*, **81**, 196–200.
Gullion, T., Baker, D.B. and Conradi, M.S. (1990) *J. Magn. Reson.*, **89**, 479–484.
Hardy, E.H., Detken, A. and Meier, B.H. (2003) *J. Magn. Reson.*, **165**, 208–218.
Heise, B., Leppert, J., Ohlenschläger, O., Görlach, M. and Ramachandran, R. (2002) *J. Biomol. NMR*, **24**, 237–243.
Hing, A.W., Vega, S. and Schaefer, J. (1992) *J. Magn. Reson.*, **96**, 205–209.
Hong, M. (1999) *J. Biomol. NMR*, **15**, 1–14.
Hong, M. and Griffin, R.G. (1998) *J. Am. Chem. Soc.*, **120**, 7113–7114.
Hwang, T., van Zijl, P.C.M. and Garwood, M. (1998) *J. Magn. Reson.*, **133**, 200–203.
Jaroniec, C.P., Filip, C. and Griffin, R.G. (2002) *J. Am. Chem. Soc.*, **124**, 10728–10742.
Leppert, J., Heise, B., Görlach, M. and Ramachandran, R. (2002) *J. Biomol. NMR*, **23**, 227–238.
Leppert, J., Heise, B., Ohlenschläger, O., Görlach, M. and Ramachandran, R. (2003) *J. Biomol. NMR*, **26**, 13–24.
Leppert, J., Ohlenschläger, O., Görlach, M. and Ramachandran, R. (2004a) *J. Biomol. NMR*, **29**, 167–173.
Leppert, J., Urbinati, C.R., Hafner, S., Ohlenschläger, O., Swanson, M.S., Görlach, M. and Ramachandran, R. (2004b) *Nucl. Acids Res.*, **3**, 1177–1183.
Levitt, M.H. (2002) *Encyclopedia of NMR*, **9**, 165–196.
Levitt, M.H., Freeman, R. and Frenkiel, T. (1983) *Adv. Magn. Reson.*, **11**, 47–110.
Michal, C.A. and Jelinski, L.W. (1997) *J. Am. Chem. Soc.*, **119**, 9059–9060.
Naito, A., Nishimura, K., Kimura, S., Tuzi, S., Aida, M., Yasuoka, N. and Saito, H. (1996) *J. Phys. Chem.*, **100**, 14995–15004.
Nishimura, K., Fu, R. and Cross, T.A. (2001) *J. Magn. Reson.*, **152**, 227–233.
Pauli, J., Baldus, M., von Rossum, B., de Groot, H. and Oschkinat, H. (2001) *Chembiochem*, **2**, 272–281.
Ranum, L.P.W. and Day, J.W. (2004) *Am. J. Hum. Genet.*, **74**, 793–804.
Riedel, K., Leppert, J., Ohlenschläger, O., Görlach, M. and Ramachandran, R. (2004a) *Chem. Phys. Lett.,* **395**, 356–361.
Riedel, K., Leppert, J., Häfner, S., Ohlenschläger, O., Görlach, M. and Ramachandran, R. (2004b) *J. Biomol. NMR*, in press.
Rienstra, C.M., Hohwy, M., Hong, M. and Griffin, R.G. (2000) *J. Am. Chem. Soc.*, **122**, 10979–10990.
Sinha, N., Schmidt-Rohr, K. and Hong, M. (2004) *J. Magn. Reson.*, **168**, 358–365.
Sun, B.-Q., Rienstra, C.M., Costa, P.R., Willamson, J.R. and Griffin, R.G. (1997) *J. Am. Chem. Soc.*, **119**, 8540–8546.
Szeverenyi, N.M., Sullivan, M.J. and Maciel, G.E. (1982) *J. Magn. Reson.*, **47**, 462–475.
Tycko, R., Pines, A. and Guckenheimer, J. (1985) *J. Chem. Phys.*, **83**, 2775–2802.
Van Eck, E.R.H.and Veeman, W.S. (1994) *J. Magn. Reson. A*, **109**, 250–252.
Weldeghiorghis, T.K. and Schaefer, J. (2003) *J. Magn. Reson.*, **165**, 230–236.
Wijmenga, S.S. and van Buuren, B.N.M. (1998) *Prog. Nucl. Magn. Reson. Spectrosc.*, **32**, 287–387.